

Electrodynamic Tether at Jupiter. II. Fast Moon Tour after Capture

Juan R. Sanmartin, Mario Charro, Enrico C. Lorenzini, Henry B. Garrett, Claudio
Bombardelli, and Cristina Bramanti

Abstract-- An electrodynamic tether mission at *Jupiter*, following capture of a spacecraft (SC) into an equatorial, highly elliptical orbit with perijove at about 1.3 times the Jovian radius, is discussed. Repeated application of propellantless Lorentz drag on a spinning tether, at the perijove vicinity, can progressively lower the apojove at constant perijove, for a tour of *Galilean* moons. Electrical energy is generated and stored as the SC moves from an orbit at 1:1 resonance with a moon, down to resonance with the next moon; switching tether current off, stored power is then used as the SC makes a number of flybys of each moon. Radiation dose is calculated throughout the mission, during flybys and moves between moons. The tour mission is limited by both power needs and accumulated dose. Three-stage apojove lowering down to *Ganymede*, *Io* and *Europa* resonances would total less than 14 weeks, while 4 *Ganymede*, 20 *Europa*, and 16 *Io* flybys would add up to 18 weeks, with the entire mission taking just over 7 months, and the accumulated radiation dose keeping under 3 Mrad (Si) at 10 mm *Al* shield thickness.

Index terms—Bare electrodynamic tether, Propellantless space propulsion, Planetary exploration, Jovian mission design.

The work by Sanmartin and Charro was supported by the European Space Agency under contract 19696/06/ and the Spanish Ministry of Science and Technology under Grant ESP2004-01511.

J. R. Sanmartin and M. Charro are with the Department of Applied Physics, School of Aeronautical Engineering, Universidad Politécnica de Madrid, 28040 Madrid, Spain

E.C. Lorenzini is with the Department of Mechanical Engineering, University of Padova, Padova, Italy

H.B. Garrett is with the Jet Propulsion Laboratory, California Institute of Technology

C. Bombardelli and C. Bramanti are with the Advanced Concepts Team, ESTEC, European Space Agency, Noordwijk, Netherlands

1. INTRODUCTION

The Jovian mission discussed here arises from a concept involving an electrodynamic (ED) bare tether to tap *Jupiter's* rotational energy for both propulsion and power. The (circular, equatorial) stationary orbit is close to Jupiter, at radius $a_s \approx 2.24 R_J$, because of both fast rotation and low density of the planet; the large Jovian magnetic field \bar{B} then allows plasma to corotate with the planet also beyond that orbit. The positions of perijove and apojove in elliptical prograde orbits relative to the stationary orbit, which lies at an energy maximum in the orbit/planet-spin interaction, might be exploited to conveniently make the induced Lorentz force to be drag or thrust, while generating power and navigating the system. The dense-plasma *Io* torus, lying well beyond the stationary orbit, could in principle allow tether thrusting [1].

The capture operation was analyzed in previous work [2]. Design parameters such as (tape) tether length L and thickness h , and perijove radius r_p , faced opposite constraints. Capturing a full SC mass M_{SC} several times its tether mass m_t requires a low perijove and a high $L^{3/2}/h$ ratio. But tether bowing, and tensile stress considerations arising from the tether spin required by the low gravity gradients and high lateral Lorentz forces at Jupiter, place a bound on the ratio $L^{5/2}/h$. Also, maximum tether temperature scales as $L^{3/8}$. In addition, both tether temperature and bowing are greater the closer to Jupiter is the perijove.

Capture required the electrodynamic drag to make a work $|W_C|$ exceeding the positive energy in the incoming hyperbolic orbit. The greater that work, the lower apojove radius and eccentricity in the first orbit following capture. In a preliminary design, a reinforced *Al* tape 50 km long and 0.05 mm thick, coated for a thermal emittance $\varepsilon_t \approx 0.8$ and spinning with about 12 minutes period, i) satisfies all constraints and ii) captures a spacecraft with full mass over three times m_t at a $1.3 R_J$ perijove, with $|W_C|$ twice the excess hyperbolic energy of a Hohmann transfer. We will use this tape as reference tether for numerical considerations. No characteristic dimensionless number involves the tape width; the SC mass will just scale up with width in a range allowing from about 0.2 to 5 metric tons. A 3 cm wide tape will be considered wherever choosing a definite mass is convenient, m_t then being 202 kg and M_{SC} about 650 kg [2].

In the present work we analyze closed-orbit evolution after capture, for a Galilean moon tour under repeated Lorentz force, which requires no propellant and no independent power supply; alternative missions after capture (acquiring low circular orbits around Jupiter and around moon Io) will be analyzed in work to follow. If current is on along the arc where the Lorentz force is drag, as the spacecraft nears perijove, the apojove radius r_a will be reduced. Further reductions will occur at successive perijove passes, resulting in a series of elliptical orbits with common perijove and decreasing eccentricities, with changes in the perijove position being small, second-order effects

With the Lorentz force only acting around perijove, the energy per unit mass ε of the incoming hyperbolic orbit and following elliptical orbits only depends on eccentricity e ,

$$\varepsilon = \frac{-\mu_J}{2r_p}(1-e), \quad (1)$$

where μ_J is Jupiter's gravitational parameter. We assume that the hyperbolic eccentricity, $e_h = 1 + r_p v_\infty^2 / \mu_J$ is just above unity; in case of a Hohmann transfer ($v_\infty \approx 5.64$ km/s), we would have $e_h - 1 \approx 0.018 r_p / R_J$. Also, as we will recall, the S/C could be barely captured; this leads to an energy balance, from Eq. (1),

$$\frac{-W_c}{M_{SC} v_\infty^2 / 2} = \frac{-\Delta \varepsilon}{v_\infty^2 / 2} = \frac{-\Delta e}{e_h - 1} = O(1). \quad (2)$$

The orbit is thus hardly affected locally, allowing to consider a parabolic ($e = 1$) orbit throughout capture. As the eccentricity decrement in the following perijove passes will be found to be also small, calculations will be here carried out as if eccentricity, though different from unity, was kept constant during each pass. The decrement Δe at fixed e is given by an equation similar to (2),

$$\frac{2W_{d,e}}{m_t v_\infty^2} = \frac{M_{SC}}{m_t} \frac{\Delta e}{e_h - 1}, \quad (3)$$

where $W_{d,e}$ is the drag work.

Propulsive performance is heavily dependent on orbit geometry as well as on ambient conditions, namely electron plasma density N_e , field \bar{B} , and motional electric field $\bar{E}_m = \bar{v}' \times \bar{B}$, where $\bar{v}' \equiv \bar{v} - \bar{v}_{pl}$ is the SC velocity relative to the corotating plasma. A simple no-tilt, no-offset dipole \bar{B} model, $B = B_s a_s^3 / r^3$ ($B_s \approx 0.38$ Gauss), will do in our analysis [3]. We shall use the *Divine-Garrett* model of the thermal Jovian plasma in the plasmasphere, which is then longitude-independent; only the plasma density profile, which has a simple analytical representation, is involved in the calculations [4].

Lowering the orbit apojove through a series of perijove passes is considered in Sec. 2. In Sec.3 we discuss using the tether to serve as its own power source by having an electric load plugged in; a large energy could be tapped (both used locally and stored for

later use) from the big power developed during SC capture and following high-current operations, with negligible effect on its dynamics. Radiation dose through the successive orbits places a limit on post-capture operation, with the GIRE radiation model used in Sec. 4 to evaluate accumulated dose throughout [5]. Section 5 deals with the design of a tour of Galilean moons.

2. LOWERING THE APOJOVE

The Lorentz force on a bare tether involves the length-averaged current I_{av} which depends on impedances in the tether circuit. The tether would spin in the equatorial orbital plane, perpendicular to the magnetic field, with hollow cathodes at both ends taking active turns as each end becomes cathodic; their contact impedance is entirely negligible. We shall also neglect both the radiation impedance for current closure in the Jovian plasma (indeed negligible at Earth) and any power-output impedance, which is discussed in the next section. The average tether current will then lie between extreme values, one corresponding to no ohmic effects, the other to ohmic-limited current.

The instantaneous Lorentz power for a general elliptical orbit reads

$$\dot{W} = \bar{v} \cdot \bar{F}_L = v \bar{u}_t \cdot (-I_{av} \bar{u} \times L B \bar{k}) \quad (4)$$

where \bar{u}_t , \bar{u} , \bar{k} are unit vectors along SC velocity, tether line from cathode to anode, and magnetic field (pointing south at the equator, $\bar{B} = -B \bar{k}$), respectively. The current is normalized with the short-circuit current as maximum possible value,

$$I_{av} \equiv i_{av} \sigma_c w h E_m, \quad (5)$$

where σ_c is tether conductivity and E_m is the projection of the electric field \bar{E}_m along the tether,

$$E_m \equiv \bar{E}_m \cdot \bar{u} = v' B \cos \varphi, \quad (6)$$

with φ the angle between tether and field \bar{E}_m . We can now write

$$(\bar{u} \times \bar{u}_t) \cdot \bar{k} = -\sin(\varphi + \alpha_E) \quad (7)$$

where α_E is the angle between \bar{E}_m and the velocity \bar{v} .

Averaging over angle φ at fixed SC position gives

$$\langle \dot{W} \rangle = -\sigma_c whLB^2 v v' \sin \alpha_E \langle i_{av} \cos^2 \varphi \rangle, \quad (8)$$

where we used the vanishing of the average $\langle i_{av} \cos \varphi \sin \varphi \rangle$, arising from both Eq.(6)

and the dependence $i_{av} \equiv i_{av}(E_m)$ recalled below. Since \bar{v}' and \bar{E}_m are perpendicular

to each other, and using conservation of angular momentum $r \bar{v} \cdot \bar{u}_\theta = r_p v_p$ where

θ is true anomaly and \bar{u}_θ is the transversal unit vector, we can write

$$v v' \sin \alpha_E = v \bar{v}' \cdot \bar{u}_t = \bar{v} \cdot (\bar{v} - \Omega_J r \bar{u}_\theta) = v^2 - \Omega_J r_p v_p, \quad (9)$$

in Eq. (8). We next integrate the power over the time Δt in the drag arc,

$$W_{d,e} = \int_{\Delta t} \langle \dot{W} \rangle dt = 2 \int_{r_p}^{r_u} \frac{\langle \dot{W} \rangle dr}{dr/dt},$$

taking v^2 from the energy equation

$$v^2 = \mu_J \left(\frac{2}{r} - \frac{1-e}{r_p} \right), \quad (10)$$

and using $r^2 d\theta/dt = r_p v_p$ and the orbit equation $1 + e \cos \theta = (1 + e) r_p / r$, to determine dr/dt .

Using then Eq.(3), we finally find the decrement Δe per orbit,

$$\frac{-\Delta e}{e_h - 1} = \frac{m_t}{M_{SC}} \tilde{B}_s^2 S_e \left(\frac{r_p}{R_J}, \Lambda, e \right), \quad (11)$$

$$S_e \equiv \tilde{r}_M^{8/3} \int_1^{\tilde{r}_u} \frac{d\tilde{r}}{\tilde{r}^6} \frac{2\tilde{r}_M - \tilde{r} \left[\sqrt{2(1+e)} + (1-e)\tilde{r}_M \right]}{\sqrt{2(\tilde{r}-1)} \sqrt{1+e - (1-e)\tilde{r}}} < 2i_{av} \cos^2 \varphi >, \quad (12)$$

$$\tilde{B}_s^2 \equiv \frac{\sigma_c B_s^2 a_s v_s}{2^{5/6} \rho_t v_\infty^2} \approx 2.11, \quad (13)$$

for aluminum tape and Hohmann transfer. In the above we wrote

$$\tilde{r} \equiv r/r_p, \quad r_M(r_p) \equiv a_s \sqrt{2a_s / r_p}, \quad (14a, b)$$

and used the parabolic velocity at a_s as reference velocity, $v_s \equiv \sqrt{2\mu_J / a_s} \approx 39.8$ km/s. For a range of eccentricities below 1, the upper end at the integral $\tilde{r}_u \equiv r_u / r_p$ marks the limit of the drag arc, where the tangential component of the relative velocity v_t' vanishes with the numerator in the integral. As eccentricity decreases, however, a value is reached such that r_u is the apojove radius $r_a \equiv r_p (1 + e) / (1 - e)$; for lower e values, drag acts throughout the orbit.

The dimensionless average current is an universal function $i_{av}(\hat{L})$ given in Ref. 2. In case of negligible ohmic effects, bare-tether analysis shows the tether biased positive throughout its length, and the average current to be 2/5 of the OML current collected by the tether if at uniform bias $E_m L$,

$$I_{av}(OML) = \frac{2}{5} \frac{2wL}{\pi} eN_e \sqrt{\frac{2eE_m L}{m_e}}. \quad (15)$$

In general, $I_{av} / \sigma_c w h E_m \equiv i_{av}$ is found to be a function of the ratio $I_{av}(OML) /$

$\sigma_c w h E_m \equiv 3 \hat{L}^{3/2} / 10$, with \hat{L} as given in Ref. 2,

$$\hat{L}(\cos \varphi, \tilde{r}, e, \Lambda, \tilde{r}_M) \equiv \frac{\Lambda \tilde{r}^{7/6} / |\cos \varphi|^{1/3} \tilde{r}_M^{4/9}}{\left[\tilde{r}_M^2 + \tilde{r}^3 - \left(\sqrt{2(1+e)} + \frac{1-e}{2} \tilde{r}_M \right) \tilde{r}_M \tilde{r} \right]^{1/6}} \left(\frac{N_e}{N_s} \right)^{2/3}, \quad (16)$$

$$\Lambda \equiv \frac{2^{49/18}}{(3\pi)^{2/3}} \left(\frac{N_s}{\sigma_c h} \right)^{2/3} \frac{eL}{\left(m_e v_s B_s \right)^{1/3}} \approx 0.200 \frac{L}{50km} \left(\frac{0.05mm}{h} \right)^{2/3}, \quad (17)$$

where we use the conductivity of aluminum, the (no-tilt) Divine-Garrett density model at the equator, and the density $N_s = 1.44 \times 10^2 \text{ cm}^{-3}$ at a_s [4],

$$N_e = \frac{4.65}{3} \exp\left(\frac{7.68 R_J}{r}\right) \Rightarrow \frac{N_e}{N_s}(\tilde{r}, \tilde{r}_M) = \exp\left(2.72 \frac{\tilde{r}_M^{2/3}}{\tilde{r}} - 3.43\right). \quad (18)$$

For $e = 1$, Eq. (11) recovers results in Ref. 2 (with $\Delta e = e_1 - e_h$),

$$\frac{-\Delta e}{e_h - 1} = \frac{m_t}{M_{SC}} \tilde{B}_s^2 S\left(\frac{r_p}{R_J}, \Lambda\right). \quad (11')$$

Figure 1 shows S_e versus e for $r_p = 1.3 R_J$ and several Λ values. S_e is indeed nearly independent of eccentricity ($S_e \approx S$ or $W_{d,e} \approx W_C$) except at small e . We find drag acting over the entire orbit if $r_a < 2.05 R_J$ for $r_p = 1.3 R_J$ or $e < 0.22$, which falls in the eccentricity range showing a rapid increase of S_e in Fig. 1; for $r_p = 1.1 R_J$ and $r_p = 1.5 R_J$, we find full orbit drag for $e < 0.29$ ($r_a < 2.0 R_J$) and $e < 0.17$ ($r_a < 2.1 R_J$), respectively. We may thus use (11') throughout, the e -range of interest for the moons tour in Sec. 5 excluding small e values. Note that capture requires a minimum decrement $|\Delta e| = e_h - 1$, which is proportional to v_∞^2 , the corresponding mass ratio then depending on the hyperbolic excess velocity too; on the other hand, given the mass ratio, Δe is independent of v_∞ .

The limit $\Lambda \rightarrow \infty$, and $i_{av} \rightarrow 1$, corresponds to dominant ohmic effects, which Eq. (19) shows requiring impracticably high values of the tape ratio $L/h^{3/2}$. Small Λ values

for reasonably practical tapes, such as our reference design tape, correspond to negligible ohmic effects, with $i_{av} \approx I_{av}(OML) / \sigma_c E_m wh = 0.3 \hat{L}^{3/2}$, and

$$\frac{-\Delta e}{e_h - 1} = \frac{m_t}{M_{SC}} \times 0.15 \left(\frac{L}{50km} \right)^{3/2} \frac{0.05mm}{h} \Sigma \left(\frac{r_p}{R_J} \right). \quad (11'')$$

The function Σ , as given in Ref. 2, is used in Fig. 2 to represent the eccentricity decrement vs perijove radius for the reference 50 km long, 0.05 mm thick tape, and two values of the mass ratio roughly corresponding to decrements $\Delta e = 1 - e_h$ and $2(1 - e_h)$.

We can now readily describe orbit evolution in terms of the number of successive perijove passes. For Hohmann transfer and the 50 km, 0.05 mm aluminum reference tape with capture at $1.3 R_J$ perijove leads to $e_h \approx 1.02$, $e_1 \approx 0.98$ and $\Delta e \approx -0.04$ at not too small e . A series of passes at fixed perijove, with repeated small decrements in eccentricity, would then result in a sequence of e values, 0.98, 0.94, 0.90, 0.86, 0.82, 0.78, 0.74, 0.70, ... The orbital period of the SC after each perijove pass is $\tau_{orb} \propto [r_p / (1 - e)]^{3/2}$, yielding a corresponding sequence of periods, 64.8, 12.4, 5.8, 3.5, 2.4, 1.78, 1.37, 1.13, ... days. Note, however, that flyby operations to be discussed in Sec. 5 will modify that sequence.

3. POWER BUDGET

During capture, a very large amount of energy would be taken from the orbital motion of the SC into the tether electric circuit, and ultimately transformed into thermal energy of the tether, to be radiated away as discussed in Ref.2. From Eq.(2), with $\Delta e \approx -2(e_h - 1)$, we have

$$\frac{|W_C|}{M_{SC}} = v_\infty^2 \approx \frac{8.84 MWh}{10^3 kg} \quad (19)$$

or 5.75 MWh for the 650 kg SC corresponding to the 3cm-wide reference tape. Clearly, a small fraction of that energy could be taken by electric loads at the tether ends, with negligible effect on tether current and thus on the dynamics of capture. A small part of that energy could be used during capture, but a much greater part, E_{st} , might be saved/stored in batteries or regenerative fuel cells, for later use (for instance, for powering electrical propulsion if convenient). Similar results apply for each of the successive perijove passes.

The saved energy would be basically limited by the mass of the storing device. Storing a 0.5 per cent energy fraction, or about $E_{st} \sim 30$ kWh, could provide 250 W power during 120 hours. The cycle life of the batteries, as considered in Sec. 5, would be low, say a few tens of cycles, possibly allowing use of batteries with specific energy as high as 0.5 kWh/kg, for a mass of 60 kg. In case of a regenerative fuel-cell, both cell and fuel (hydrogen *plus* required oxygen) masses contribute to system mass. The ideal specific power of the fuel is about 4.3 kWh/kg but the masses of storage tanks and inefficiencies would make 2 kWh/kg a more realistic figure, yielding a fuel related mass of 15 kg. With a cell specific power of order 100 W/kg, the overall storage mass would be under 20 kg. Fuel storage could be a main issue [6], [7].

Power decays rapidly away from its peak at the perijove, which is a result of the density profile being very steep near Jupiter, most of the energy decrease $|W_C|$ occurring in a short orbit arc. Over most of the plasmasphere the Lorentz force has thus a negligible effect on the SC dynamics. Nonetheless, the tether can generate power for local use over intermediate orbit segments, saving fuel-cell power for the regions outside the denser parts of plasmasphere and torus. Consider the average power given by Eq. (8) at capture ($e = 1$) and negligible ohmic effects (small Λ),

$$\begin{aligned}
\frac{|\langle \dot{W} \rangle|}{m_t} &= \frac{0.2 N_s}{\rho_t h} e v_s B_s L \sqrt{\frac{e v_s B_s L}{m_e}} \left(\frac{a_s}{r} \right)^{9/2} \frac{N_e}{N_s} \frac{|\tilde{r}_M - \tilde{r}|}{2^{1/4} \tilde{r}^{3/4} \sqrt[4]{\tilde{r}_M^2 - 2\tilde{r}_M \tilde{r} + \tilde{r}^3}} \\
&\approx 0.884 \frac{\tilde{r}_M^3}{\tilde{r}^{21/4}} \frac{|\tilde{r}_M - \tilde{r}|}{(\tilde{r}_M^2 - 2\tilde{r}_M \tilde{r} + \tilde{r}^3)^{1/4}} \times \frac{N_e}{N_s} (\tilde{r}, \tilde{r}_M) \frac{kW}{kg}. \quad (20)
\end{aligned}$$

This local power per unit tether mass is represented in Fig. 3.

Results in Fig. 3 correspond to zero load impedance. Using the tether in a generator mode, over intermediate orbit segments with current along with the hollow cathodes on, requires a load impedance comparable to the impedance of OML current collection. Although the Lorentz power taken from the SC motion would be very small (when compared with the power produced during high-current operations, thus having negligible effect on orbit dynamics), the load would take a fraction (the generator efficiency η_g) of order unity of such power. For negligible ohmic effects one finds *i*) $\eta_g = 10/19$ for the conditions of maximum load power, and *ii*) the Lorentz power itself smaller than its value for no load impedance by a factor $\sqrt{3/5} \times 19/15 \approx 0.589$ [8]. The load power attained under optimal conditions would then be less than as shown in Fig. 3 by a factor $0.589 \times 10/19 = 0.31$. Yet, as far as $r = 2.4 r_p = 3.12 R_J$ for the 1.3 R_J perijove, a maximum power per unit tether mass of 0.31×5 w/kg or about 300 w might be attained with the 202 kg, 3cm-wide reference tape.

4. RADIATION DOSE

As regards radiation, there exist two basic modifications of the **D/G** model, which had originally covered the magnetic shell range $1.09 < L < 16$. Later analysis of data from the Galileo *Energetic Particle Detector* led to modifications over the range $8 < L < 16$ and the development of the so called **GIRE** (*Galileo Interim Radiation Electron*) model [5]. **GIRE** somewhat reduces the dose rate, as compared with the **D/G** model,

near the Europa and Ganymede orbits but leaves the $L < 8$ range (dominant as regards radiation) unmodified, and thus has only a moderate relative effect on the dose per orbit for orbits that reach very close to Jupiter. A second modification of the **D/G** radiation model covers the $L < 4$ range, well inside the inner magnetosphere. It was based on a recent analysis that fit the synchrotron emission data from Earth-based measurements. It primarily affects relativistic (multi-Mev) electron energies and the electron flux only in the narrow range $2 < L < 2.3$, and thus will be ignored here [9].

A simple benchmark for estimating radiation effects over the orbit evolution of the tethered spacecraft is the calculation of dose over a parabolic capture orbit. Calculations were carried out starting at $15 R_J$, moving inwards to perijove, and then ending at $15 R_J$, using the GIRE radiation model. Figure 4 shows dose/depth curves for both $1.2 R_J$ and $1.5 R_J$ capture perijoves, at 200° and 290° West Longitudes in standard SIII coordinates (roughly corresponding to minimum and maximum of dose).

Dose involves both fluence and the stopping power by a specified shielding material, typically aluminum; for any given shield-thickness, incident particles below some energy will not come out at the opposite side of the shield. As a result, radiation dose, in terms of a reference material (silicon) placed behind the shield, will decrease with increasing shield thickness. A standard shielding configuration was used in the calculation of radiation dose, the generic code involving an aluminum spherical shell for all 4π steradians.

Figure 4 shows that dose is weakly dependent on longitude, reflecting the low values of both tilt and offset of the dipole describing the magnetic field in the inner magnetosphere (ignored in our analysis of both capture and orbit evolution). Independently, at distances very close to Jupiter, dose decreases, though weakly, as the perijove is located closer and closer to the planet. Full dose over the orbit capture is

about 50 krad Si for 10 mm (or about 400 mils) shielding thickness. It appears generally accepted that electronic equipment to use in future Jovian missions will need be hardened well over 1 Mrad Si , with shield thicknesses of up to 10 mm of Al depending on the specific orbit.

If one proceeds along a sequence of orbits of decreasing apojoive, comparable values of dose per orbit result. Figure 5 shows the dose increment per orbit, for two perijove values, versus eccentricity (or equivalently, apojoive); the dose increment first increases, then exhibits a substantial decrease as e is reduced.

5. JOVIAN MOONS TOUR

The spacecraft apojoive can be lowered to any moon orbit, with a particular perijove allowing for resonance between the (elliptical) SC and the (circular) moon orbits. This would allow tangential, conveniently slow flybys of the moon. More than one perijove pass per flyby would take place for such flybys, however; we find that this rapidly increases the accumulated radiation dose. We are thus here considering non-tangential flybys at 1:1 resonance, with one perijove pass per flyby. The $1.3 R_J$ perijove, elliptical orbits at 1:1 resonances with the moons *Ganymede*, *Europa*, and *Io*, which lie at distances 15.0, 9.4, and $5.9 R_J$, have eccentricities 0.913, 0.862, and 0.779, respectively.

Figure 5 shows the radiation dose per perijove pass, at $1.3 R_J$, lying in the range $5 - 7 \times 10^4$ rads Si for 10 mm Al shield thickness, in the eccentricity range $0.78 - 1$. Taking an approximate average of 6×10^4 rads and keeping below a maximum accumulated dose of 3 Mrads Si allows up to 50 perijove passes. On the other hand, the sequence of orbits corresponding to a uniform eccentricity decrement $\Delta e = 0.04$ allows reaching the 1:1 resonances for the different moons very rapidly. This will make

for a high number of flybys. Note that the last eccentricity decrement previous to any particular resonance must be reached in two convenient steps by switching the current off appropriately over part of the drag arc, to allow for a first flyby of the respective moon. Switching off the current afterwards over the entire resonance orbit would allow repeated flybys, with the moon overtaking, each time, the slower moving SC.

We note that the large J_2 zonal harmonic coefficient in Jupiter's gravitational potential (0.01473 as against 0.00108 for the Earth) would have a small but cumulative effect on the sequence of flybys for each moon. The absidal precessions (once the nodal regressions are taken into account) for moon and flyby orbits differ by about 1.25 degrees per orbit, for Ganymede, Europa and Io cases. This will require slightly larger flyby orbits, with 1.0035 : 1 resonances. Figure 6 is a schematic of Europa's flybys showing three well-separated orbits (i.e., the 1st, 6th and 11th). The moon is encountered at successively delayed times because of the differential absidal precession that is compensated for by the slightly-increased orbital resonance as noted previously.

A tentative moon tour would involve 4 Ganymede, 20 Europa, and 16 Io flybys, for a total of 40 flybys. At an average of 6×10^4 rads S_i per flyby, it makes a total of 2.4 Mrads. In addition, two perijove passes after capture are required prior to the pass leading to the first Ganymede flyby; one and two perijove passes are required prior to passes leading to the first Europa and Io flybys, respectively. This makes a total of 0.36 Mrads S_i , the combined accumulated dose being less than 3 Mrads.

Power needs must also be considered in limiting the number of flybys; as suggested in Sec. 3, energy stored during the move down to each moon, might allow for 120 h at 250 w, for the 3-cm wide tape and 650 kg SC. Because the Europa flybys would be of the most critical interest we set its number greater than the number of flybys for Io, even

though Io's orbital period is half the Europa period; this means that the energy stored would be shared over a larger lapse of time in visiting Europa. A total of 120 h over 20 visits would still allow 6 hours per visit. We note that the primary acquisition of science data in the JUNO mission will occur over a 6 hour period centered at perijove, though science data from the just-completed perijove science will be transmitted outside this window [10].

The total duration of the mission is quite short. The three apojove lowering stages, from capture to Ganymede resonance, and later to Europa and to Io resonances, would take 86.8, 5.0, and 4.6 days, respectively, for a total of less than 14 weeks. In turn, each Io flyby takes the Io period, or about 1.77 days. Flybys for Europa and Ganymede take twice and four times as much respectively. All flybys phases would then add to a total of about 18 weeks, the entire duration of the mission being just over 7 months. The extremely frequent access of the tethered SC to the orbits of Galilean moons is to be compared to the frequency of visits in the *Galileo* mission. Galileo made 34 close encounters or flybys in almost 8 years; it thus took nearly three months on the average from one visit to the next. The price paid here is the rapid accumulation of radiation dose due to the tethered SC orbiting through the intense radiation belts near Jupiter on each moon visit.

6. CONCLUSIONS

We have analyzed an electrodynamic tether mission at *Jupiter*, following capture of a spacecraft (SC) into an equatorial, highly elliptical orbit with perijove at about 1.3 times the Jovian radius. The tethered SC can then rapidly and frequently visit Galilean moons. Repeated application of the propellantless Lorentz drag on the (spinning) tether,

at the perijove vicinity, can progressively lower the apojoive at constant perijove, for a tour of moons.

A reinforced *Al* tape-tether, 50 km long and 0.05 mm thick, coated for 0.8 thermal emittance and spinning with about 12 minutes period, can capture a spacecraft with full mass over three times its mass, taking the 1.02 hyperbolic eccentricity of a Hohmann transfer down to a first elliptical, 0.98 eccentricity, orbit. No characteristic dimensionless number involves the tape width. The SC mass just scales up with width in a range allowing from about 0.2 to 5 metric tons. A 3 cm wide tape, its mass being 202 kg and the full SC mass about 650 kg, was taken as reference tether for numerical considerations.

Electrical energy is generated and stored as the SC moves from an orbit at 1:1 resonance with a moon, down to resonance with the next moon. Switching tether current off, stored energy, allowing 120 h at 250 w power for the 3-cm wide tape and 650 kg SC, is then used as the SC makes a number of flybys of each moon, tentatively 4, 20, and 16 for *Ganymede*, *Europa*, and *Io* respectively. Because Europa flybys would be of the most critical interest we set its number greater than the number of flybys for *Io*, even though *Io*'s orbital period is half the Europa period; this means that the energy stored would be shared over a larger lapse of time in visiting Europa. A total of 120 h over 20 visits would still allow 6 hours per visit.

Radiation dose is calculated throughout the mission, during flybys and moves between moons. The tour mission is limited by both power needs and accumulated dose. Three-stage apojoive lowering down to *Ganymede*, *Io* and *Europa* resonances would total less than 14 weeks, while the *Ganymede*, *Europa*, and *Io* flybys would add up to 18 weeks, with the entire mission taking just over 7 months, and the accumulated radiation dose keeping under 3 Mrad (Si) at 10 mm *Al* shield thickness.

REFERENCES

- 1 J.R. Sanmartin and E. C. Lorenzini, "Exploration of Outer Planets Using Tethers for Power and Propulsion", *Journal of Propulsion and Power*, Vol. 21, no. 3, 2005, pp. 573-576.
- 2 J.R. Sanmartin, M. Charro, E.C. Lorenzini, H.B. Garrett, C. Bramanti and C. Bombardelli, "Electrodynamic Tether at Jupiter. I. Capture Operation and Constraints", *IEEE Transactions on Plasma Science*, to appear.
3. *Jupiter, the Planet, Satellite, and Magnetosphere*, eds. F. Bagenal, T. Dowling, and W. McKinnon, Cambridge University, 2004, Table 24.1
4. N. Divine and H.B. Garrett, "Charged particle diastributions in Jupiter's magnetosphere", *Journal of Geophysical Research* Vol. 88, no. A9, 1983, pp. 6889-6903.
5. H.B. Garrett, I. Jun, J.M. Ratliff, R.W. Evans, G.A. Clough, and R.W. McEntire, "Galileo Interim Radiation Electron Model", *Jet Propulsion Laboratory Publication* o3-006, 2003.
6. F. Barbir, L. Dalton, and T. Molter, "Regenerative Fuel Cells for Energy Storage: Efficiency and Weight Trade-offs", AIAA Paper 2003-5937, 1st *International Energy Conversion Energy Conference*, Portsmouth, VA, 17-21 August 2003.
7. C.P. García *et al.*, "Round Trip Energy Efficiency of NASA Glenn Regenerative Fuel Cell System", *NASA / TM* 2006-214054, 2006.
8. J.R. Sanmartin, M. Martinez-Sanchez, and E. Ahedo, "Bare Wire Anodes for Electrodynamic Tethers", *Journal of Propulsion and Power*, Vol. 9, no.3, 1993, pp. 353-360.

9. H.B. Garrett, S.M. Levin, S.J. Bolton, R.W. Evans, and B. Bhattacharya, "A revised model of Jupiter's inner electron belts: Updating the Divine radiation model", *Geophysical Research Letters*, Vol. 32, L04104, 2005, pp. 1-5.
10. R. Grammier, "An Overview of the JUNO Mission to Jupiter", *International Symposium on Space Technology and Science*, Kanazawa, Japan, June 4-11, 2006.

FIGURE CAPTIONS

- 1 Factor S_e in Eq. (11) for drag work per orbit versus orbit eccentricity, for $r_p = 1.3 R_J$ and several values of parameter Λ , given in Eq. (17).
- 2 Eccentricity decrement per orbit versus perijove radius for an Al 50 km long, 0.05 mm thick tape in Hohmann transfer, for two values of the mass ratio.
- 3 Lorentz-drag power per unit tether mass in w/kg units versus position along the orbit of capture, within the plasmasphere ($r < 3.8 R_J$), for two values of perijove radius and the tape in Fig. 2.
- 4 Total dose-depth curves for an equatorial and parabolic orbit of capture for perijoves at two radii and two West Longitudes (*R.W. Evans*).
- 5 Radiation dose per orbit for two perijove values and 10 mm Al shield thickness (*R.W. Evans*).
6. Schematic of flyby orbits, in Jupiter radii, of Europa showing three (well separated) encounters at orbits 1, 6 and 11. The ratio of the periods of the flyby to Europa's orbit is 1.0035:1 to account for the differential nodal precession between the spacecraft and the moon.

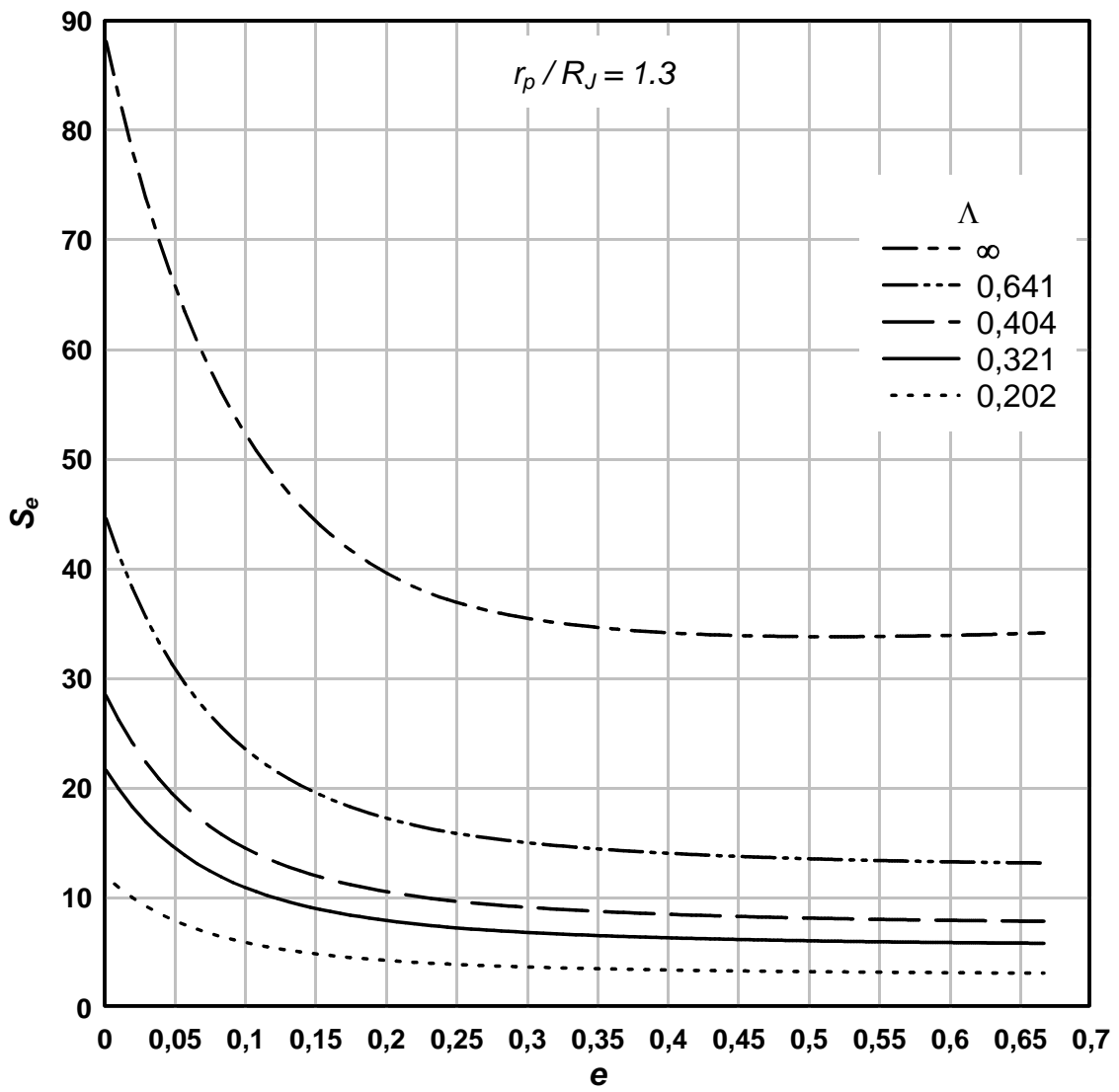


Figure 1

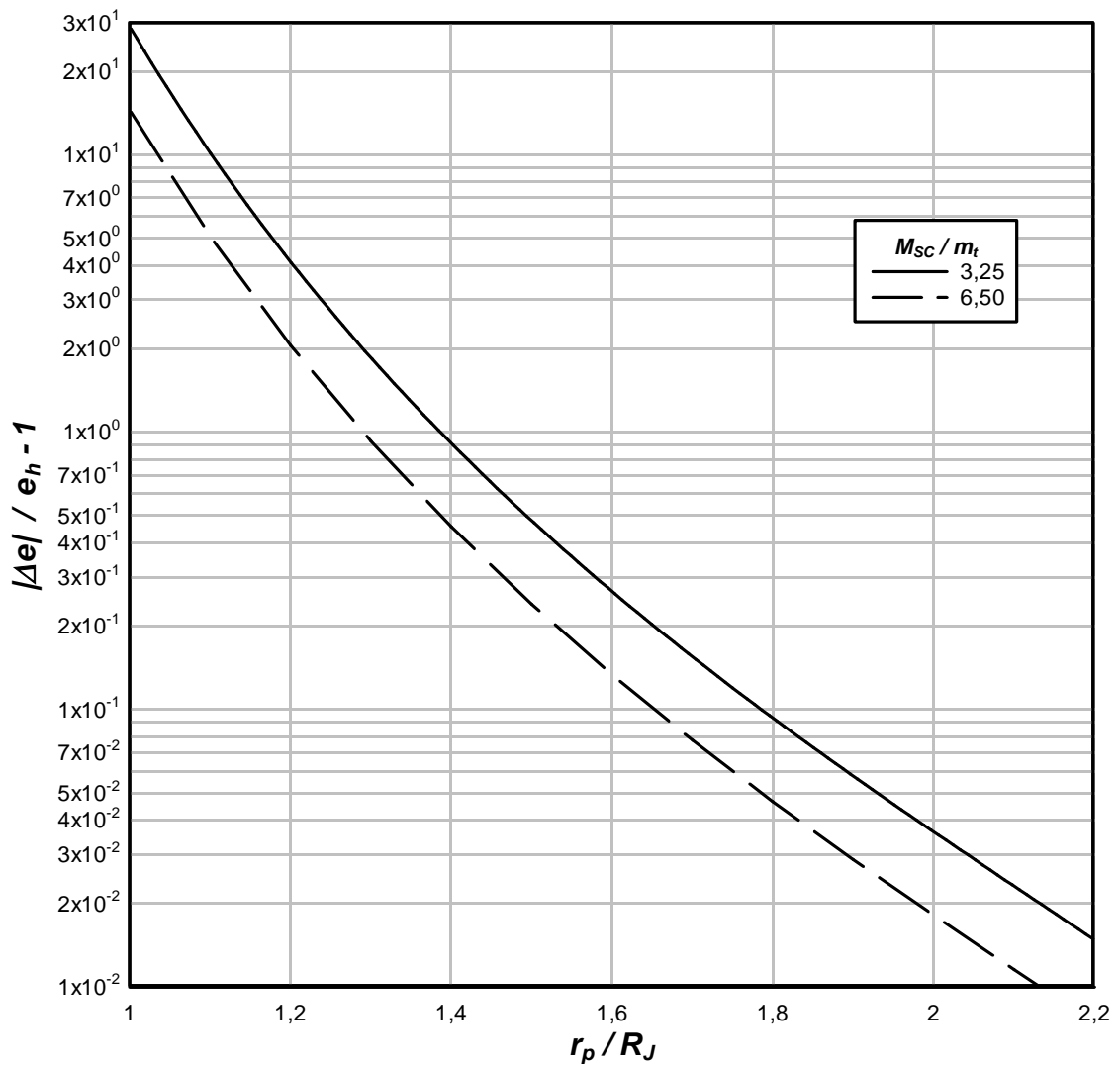


Figure 2

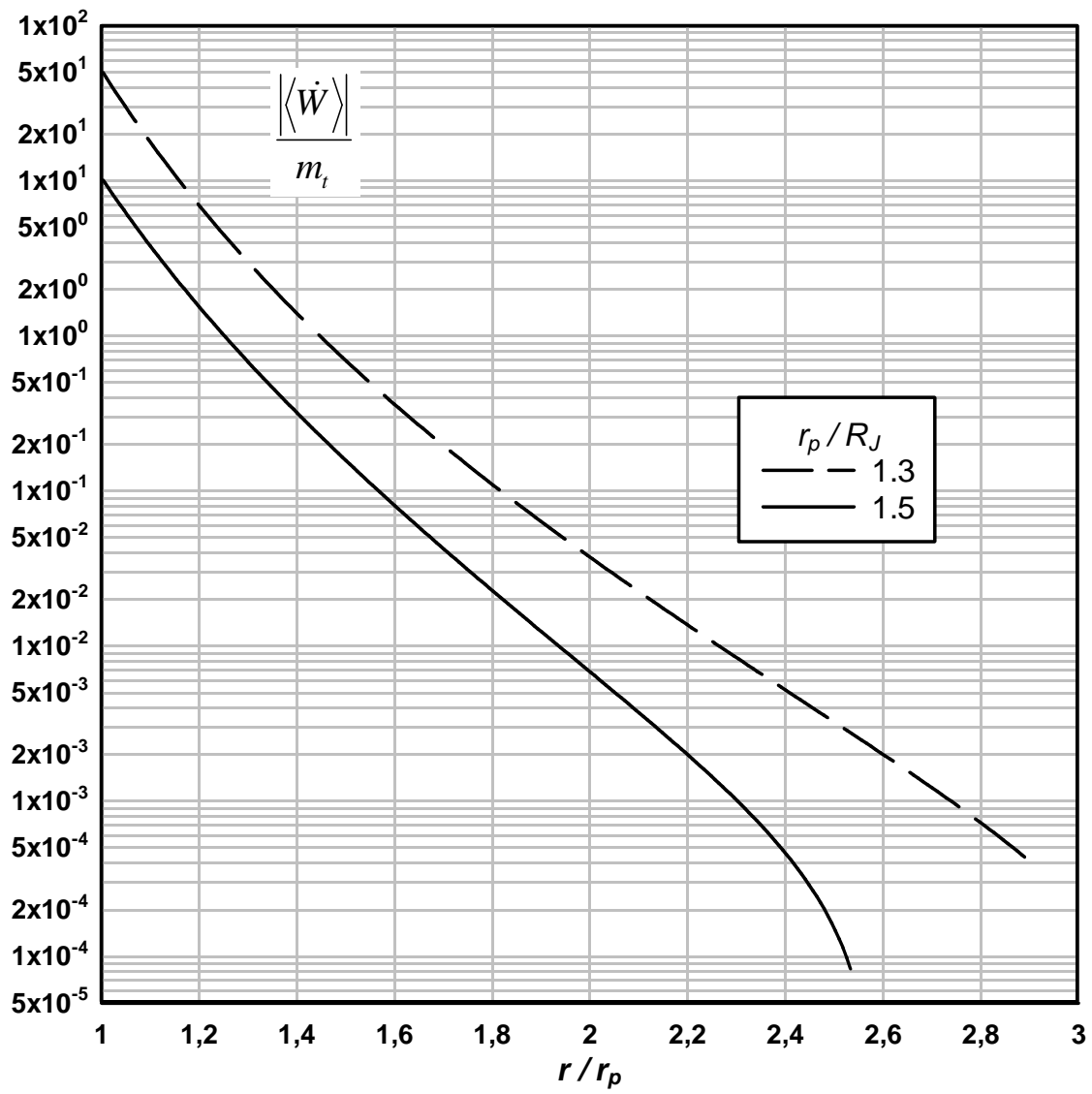


Figure 3

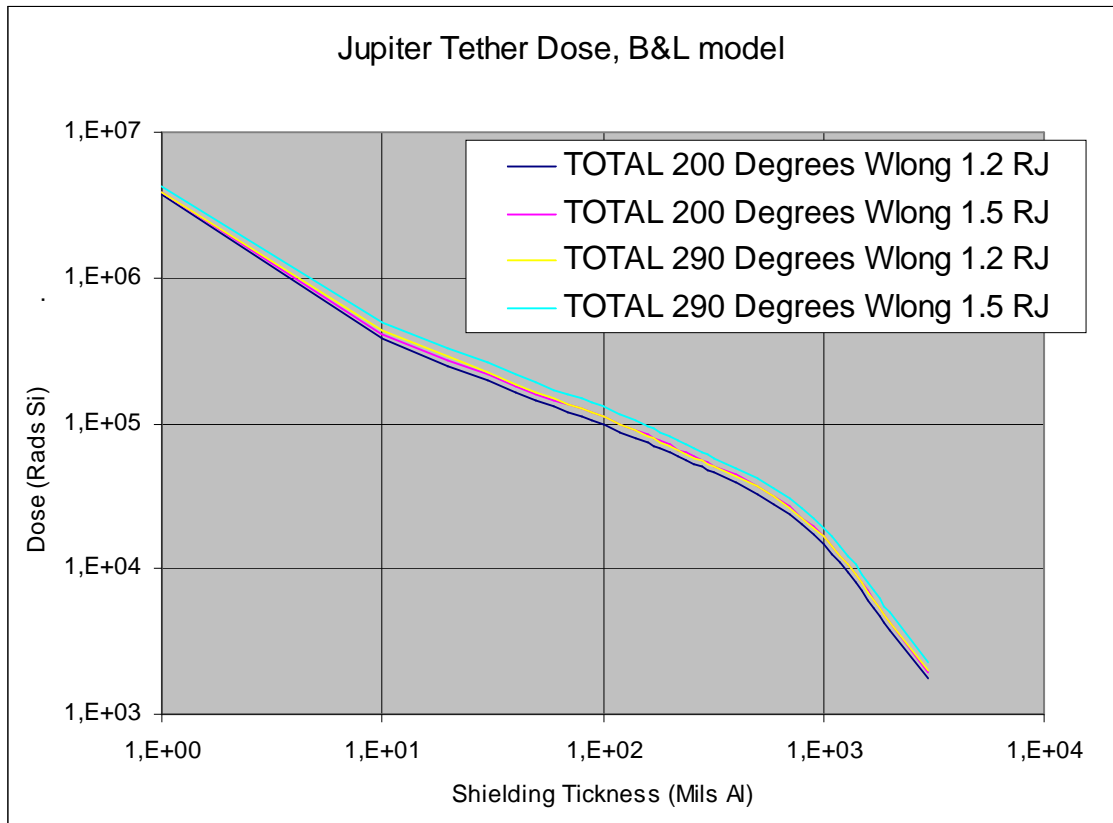


Figure 4

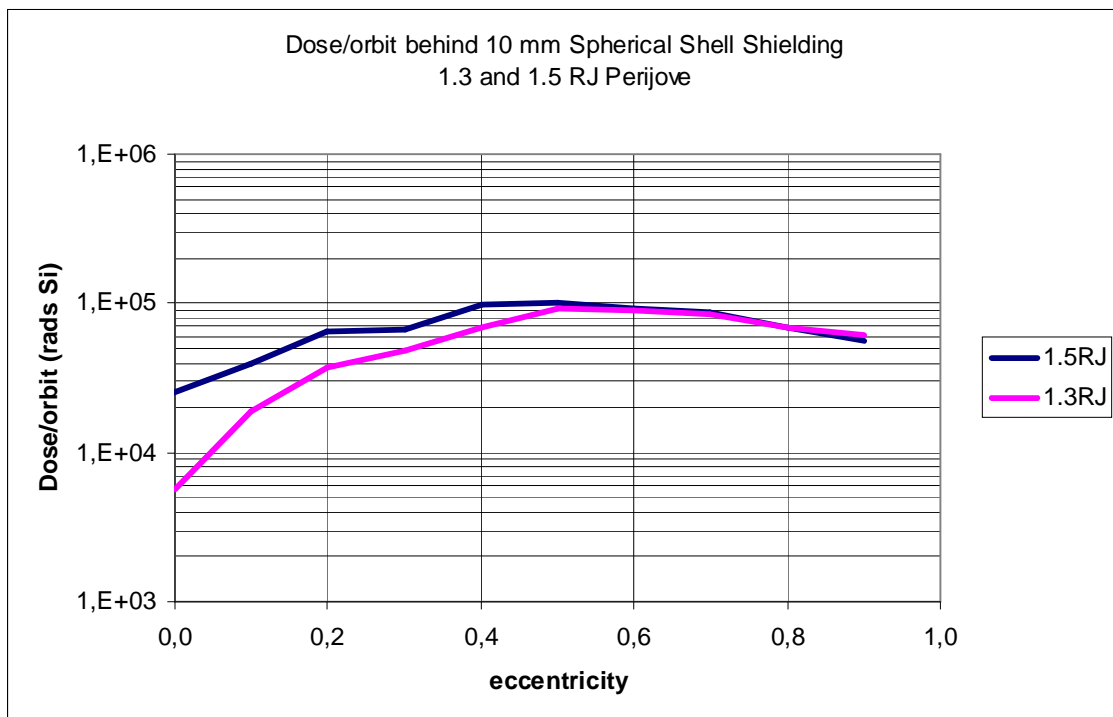


Figure 5

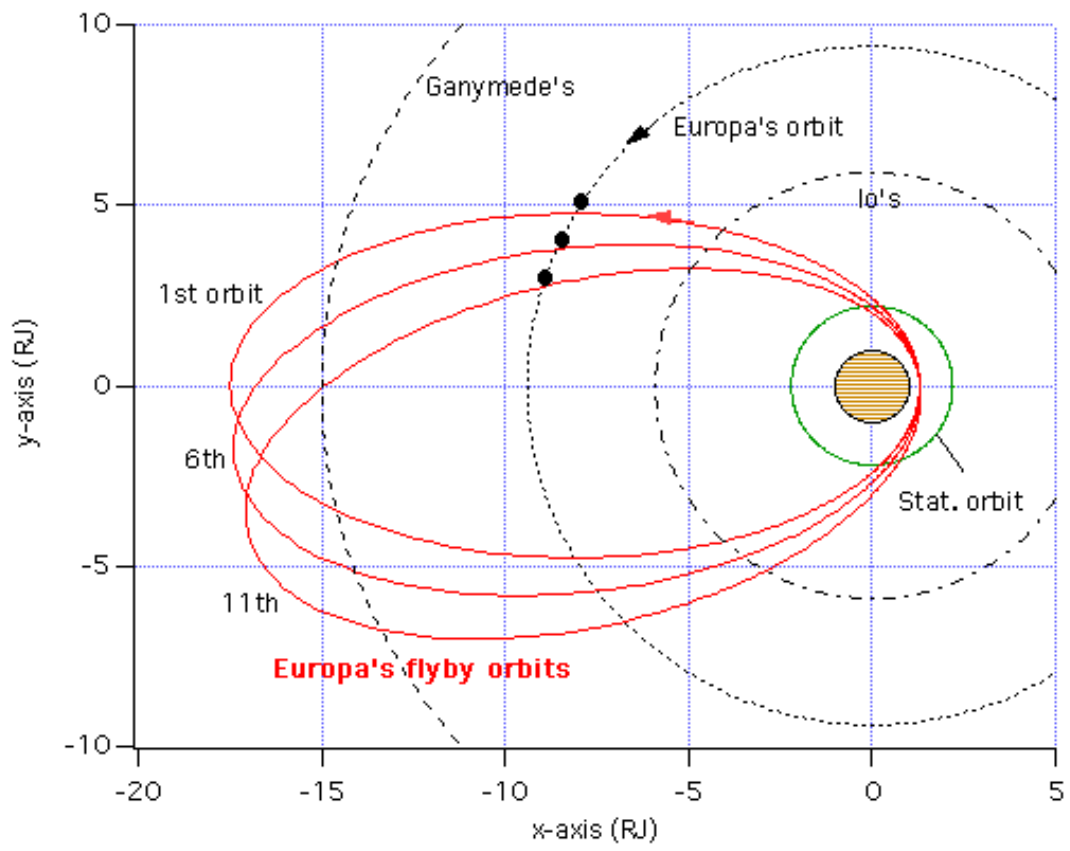


Figure 6